Multi-parametric performance evaluation of drone-based surveying for disaster risk management

Athina Silvestrou, Panayiotis Kolios, Christos Panayiotou

***Abstract*—Currently, there are many hardware (sensor) and software (algorithm) solutions designed and implemented to conduct accurate geographical surveying. Depending on the particular needs, the proper combination of hardware and software has to be selected to produce appropriate results, both with respect to quality and processing time. The recent introduction of drones (Unmanned Aerial Systems) in this domain, coupled with their increasingly automated data-collection capabilities, has spurred renewed interest in this domain due to the potential for (near) real-time, high quality, and easy data collection. In this paper we investigate novel photogrammetric approaches to collect, process and output dense clouds, orthophotos and Digital Elevation Models (DEMs) considering the aforementioned aspect (i.e. time sensitivity) in disaster risk management missions. The drone-based flight and sensing parameters are jointly investigated (including the flight altitude, camera field of view, sectorization of the field, etc.) and their effect on the total processing time and output quality are evaluated.**

***Index Terms*—survey methods, photogrammetry, UAV platform, aerial mapping, flight altitude, orthophoto**

I. Introduction

Surveying methods are currently experiencing significant revamping mainly due to the increasing computing capabilities coupled with improved equipment that has higher accuracy [1]. As a result, mapping projects over larger areas, with higher resolution and higher accuracy, and reduced computational time can be realized, as indicated in [2].

Technological advances in surveying methods have led to higher quality models with more data points of heterogeneous information. However, survey methods have mostly been employed in application domains with loose delay constraints and thus the real-time aspect has never been of primary concern. Additionally, remote data collection is in general of lower quality than the alternative terrestrial methods and thus measures need to be taken to increase accuracy [3]. The use of Ground Control Points (GCPs) as a method to correct the georeferencing errors, is a topic that received considerable interest in the literature [4] [5] [6] [7]. At least 3 GCPs are used per mission in order to minimize the image block deformations, to avoid the instability of the bundle solution and finally to ensure the creation of the 3D model [8].

In addition, drone-based surveying introduces a multiplicity of additional factors that affect both accuracy and completion times [9]. With respect to flight planning, higher travelling speeds and higher altitudes reduces data collection times at the expense of lower sensing resolution [10]. In addition, most positioning devices onboard drone platforms, are generally not able to provide location information with accuracy more than +/-5m. RTK and DRTK technology could be deployed at the expense, however, of shorter fly times and travel distances (due mainly to the increasing weight and limited available transmit power).

Another essential factor, is the sensitivity of the sensor payloads. Specifically, an accurate camera calibration is important in order to get a precise and reliable model [11] but self-calibration is not always an adequate option and alternative metric pre-calibrated cameras can be used instead [26]. The main causes that set the calibration essential, include primarily environmental factors (temperature, pressure) which may change some of the interior parameters.

Nevertheless, drone-based surveying stems as a highly favorable approach for on-time surveying especially in disaster risk management operations as exemplified above. Many methods and sensors have been considered to date as shown in [12] and drone-based approaches have unlocked capabilities that could not be possible before; especially in hard to reach areas [13].

In addition, survey solutions using aerial drone platforms, have expanded significantly in recent years [14] [15]. Clearly, drone platforms can offer sensing measurements at: a) the low capital and operating cost, b) the small weight and form factor, c) high ground resolution [8], d) their ability to deploy easily, e) the ease of capturing images/videos, and e) the ability of drones to fly at arbitrary altitudes [12] [13] enables collection of data (images/ videos) of variable accuracy depending on the mission. Importantly, drone platforms are easily programmed to address varying requirements, and thus, easily adapt to the user needs [16]. Moreover, the high spatial and temporal resolution of onboard sensors and the ability to carry multiple such sensors enable significant uptake of this technology [17].

Example scenarios include their use to monitor active volcanos, open-pit mines and many other hard-to-access areas [18]. Moreover, contributing in fields like cultural heritage, precision agriculture, drones have helped considerably in the development and to the evolution of this field [19].

In this work we investigate flight planning parameters and the image processing procedure, in order to expedite the creation of the geographic model. Specifically, we investigate:

i. How the selection of the photogrammetric method parameters can affect the total mission time (different software tools are also investigated).

A. Silvestrou, P. Kolios, and C. Panayiotou are with the Department of Electrical and Computer Engineering and the KIOS Research and Innovation Center of Excellence, University of Cyprus, {asilve01, pkolios, christosp}@ucy.ac.cy

ii. How the altitude can affect the total mission time and model quality.
iii. How the division of the area into sectors can affect the total mission time.

The rest of the paper is organized as follows; Section 2 contains related work and exemplifies the basic photogrammetry principles. Section 3 details the proposed methodology while Section 4 includes a detailed experimental analysis.

II. Background and Related Work

A. Survey sensors and methods

Survey missions include a series of steps and procedures which need to be completed in order to model an accurate state of objects on the Earth's surface [20]. The resulting geographical model can be presented as a map, a photograph, a stand-alone 2d/3d model, or event converted to CAD drawings.

As a first step, good quality data needs to be collected and a variety of sensing equipment and platforms can be used for that purpose. Broadly speaking, sensing platforms can be either terrestrial or aerial. Terrestrial equipment used in survey missions varies depending on the field and the necessary surveying quality. Location information is extracted either thought GNSS and reference stations [21] while methods of static localization and Real Time Kinematic (RTK) are most frequently used to improve location accuracy [22]. In addition, cameras, laser scanners and radar are used to collect field measurements. In a similar fashion, aerial platforms like airplanes, satellites and drones use onboard sensors including GNSS, IMU and cameras in order to collect the relevant data mainly based on a top-down view.

Depending on the type of measurements collected, different processing methods are employed. In the case of camera sensors, digital photogrammetry methods are employed to produce the desired geographical models. With terrestrial laser measurements signal processing methods are employed [23] and so is the case with radar data. The data presentation and interpretation methods based on signal processing are still in their infancy and thus their popularity is still very limited.

Nevertheless, it is important to emphasize that there is no silver-bullet solution to be followed in all survey missions. The aim of the survey, the cost, the available time and other parameters need to be considered in selecting the most appropriate survey method for each case. Figure 1 illustrates the most popular sensors/methods of survey, considering the following parameters: the area dimensions which can be covered by each sensor/method, the offered precision, the density of the given measurements, the cost and the duration of the survey procedure.

B. Terrestrial/ Aerial Photogrammetry

Photogrammetry is a technique for determining the location, the size, and the shape of object on the earth's surface, extracted only from images [24]. 3D information is captured from features on the images taken by different positions [25].

Figure 2 illustrates the data acquisition procedure for aerial photogrammetry. While the drone platform is moving along

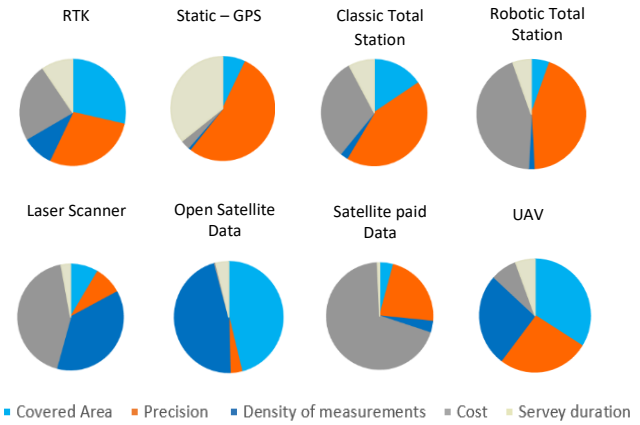

Fig. 1. The figure describes some different survey equipment and methods based on five different parameters; dimensions of the possible covered area, the offered precision, the density of the given data, the cost and the duration of the survey procedure

the field (from position P1 to position P2 in the figure) - trying to cover the whole area of interest, consecutive image captures are made. In order to compute the 3D coordinates (X, Y, Z) of every point N with coordinates (X_N, Y_N, Z_N), on the surface of Earth, each object needs to appear in at least two images, taken from different position. The distance between two consecutive images captured (distance b in Fig. 2) must have satisfactory overlap between their field of view (blue area in the figure). Importantly, the overlap greatly impacts the quality and the reliability of the end result. Let p be the forward overlap and q the lateral overlap of consecutive images. Then a value between p=75%-85% for the forward overlap (between the images) and q=65%-85% for the lateral overlap (between the flight paths) have been considered adequate enough to offer good quality results [14].

C. The photogrammetry procedure

In general, the photogrammetry procedure is separated into two main parts. Firstly, is the definition of the flight properties [6]. As indicated above, the quality of the result highly depends on the overlap of the images (p and q), in addition to the altitude (above ground/sea level), and the velocity parameters of the aircraft between acquisition points [15]. Auxiliary factors such as flight stability, the exact limits of the AOI (Area of Interest), the onboard sensors and its characteristics (RGB, thermal or multi-spectral camera), the day of the flight, the use/not use of ground control points also affects the end result [26].

The second main step of the photogrammetry procedure, is image processing. This procedure gives the final survey results of the area of interest. This step requires specific algorithms in which photogrammetric calculations are made [10]. It is important to emphasize here that careful considerations need to be made during the processing of the images to ensure the best quality.

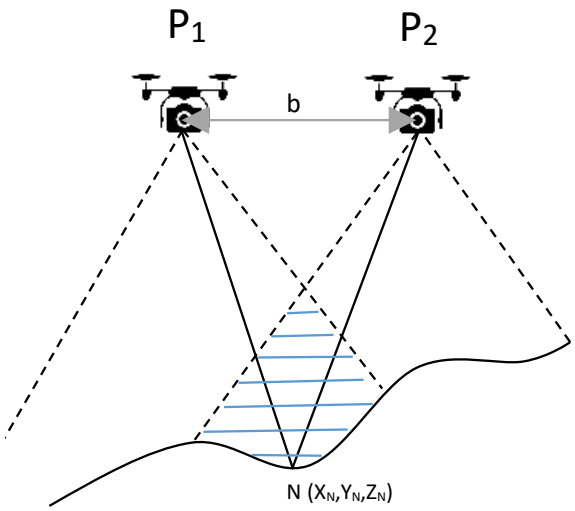

Fig. 2. The figure illustrates the basic stereo imaging approach. The two camera's positions (P1,P2) have overlapping field of view (blue area). As a result, the points existing in the overlapping area, are observed in both the images. This is the basic requirement of the estimation of the point's ground coordinates (N(XN,YN,ZN)) with the photogrammetric method.

As a first step, the way images are captured needs to be decided. Camera lenses work with a central view (the rays intersect at a central point – perspective center) (Figure 3). This type of projection generates different distortions (radial distortion etc.) which are displayed as deformations on straight and parallel lines (Figure 3). Hence, by the end of the photogrammetric procedure, the transition from a central to ortho projection (map projection) should be done (as illustrated in Figure 4). Another important aspect is that the 3rd dimension is not easily extracted from still image (i.e., 2D photos). To do so, several signal processing transformations are needed in order to obtain 3d information.

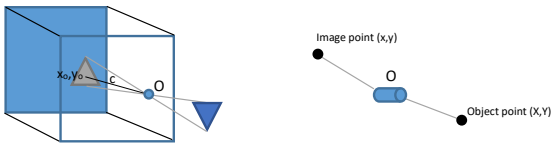

Fig. 3. The schematic on the left illustrates the way the pinhole camera is working. C is the camera constant (principal distance), O is the location of the perspective center, xo,yo is the position of the Principal Point. On the right, is illustrated the initial problem of the radial distortion where the ray which joins the coordinates of the object's point in the space, to the relative point on the image is not a continuous straight line.

To resolve the aforementioned challenges, orientation is employed (i.e., interior, exterior orientation etc.). For example, the value of the radial distortion is included in the interior orientation calculations. After the orientations are resolved, the value of essential parameters are calculated and thus the correlation of the object in the image with the object in the real world is achieved. Let r_{ij} be element (i,j) of the 3D model.

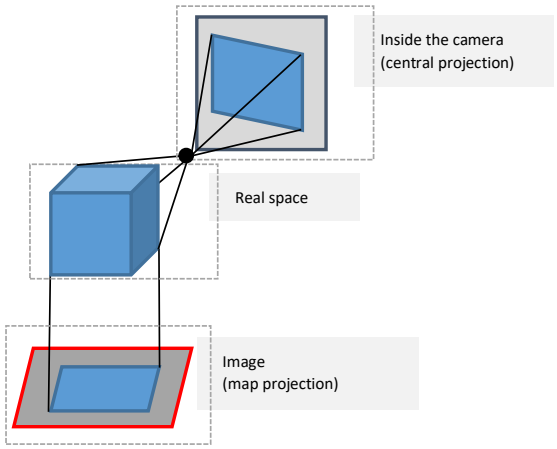

Fig. 4. The photographed object on a camera film is displayed in a central projection. This type of projection is used by the cameras but at the end of the procedure, the final result must be in an ortho (map) projection.

D. Orientation – Exterior and Interior

Orientation is defined as the computation of the altitude and position of a camera or a model in space, relative to a system of coordinate reference.

Exterior orientation of the camera, aims to define its location in the object's space (position) and its view direction (rotation) [27]. The exterior orientation helps in achieving consistency between the image and the object. The camera position is determined by the location of its perspective center and by its attitude expressed by 3 angles. So, 6 parameters need to be established. The exterior orientation of a single cone of rays, consists of:

1) The coordinates of the perspective center (Xo, Yo, Zo).
2) The camera orientation R consists of angles (ω, ϕ, κ) at the particular capture time.

These exterior parameters are shown in fig. 5.

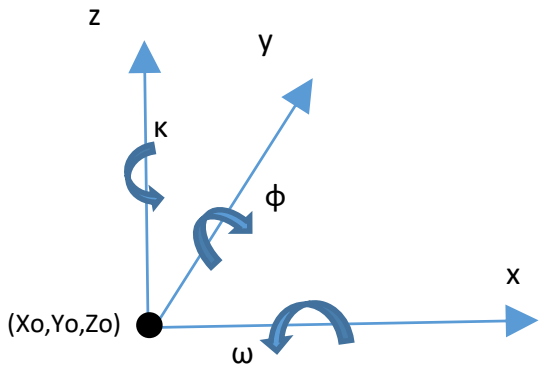

Fig. 5. This figure illustrates the elements of the exterior orientation. This elements are the perspective center coordinates (Xo,Yo,Zo) and the 3 orientation angles (ω, ϕ, κ) of the camera at the capture time.

Six parameters (i.e., unknown elements) need to be calculated by the exterior orientation. The known (measured)

parameters are simply the image coordinates (x, y) and since there are 3 unkowns (i.e., the coordinates of the point in the 3D space) the exterior orientation cannot be solved only using a single image.

Hence given a set of images that include each object more than once, the collinearly model in eq. (1) is employed. This model requires that the perspective center (X_0, Y_0, Z_0), the object point (X, Y, Z), and the relevant point on the image (x, y) must be on the same straight line (i.e., collinear) [21]. The estimated state using the collinearly model is given below:

$$\begin{bmatrix} x \\ y \\ -c \end{bmatrix} = \lambda R_{\omega\phi\kappa} \begin{bmatrix} X - X_0 \\ Y - Y_0 \\ Z - Z_0 \end{bmatrix} \quad (1)$$

where (x, y) are the object point coordinates on the image, c is the camera constant, λ is the scale, R is an orthogonal rotation matrix containing the three angles ω, ϕ, κ, (X,Y,Z) are the coordinates of the object point, and (X_0, Y_0, Z_0) are the coordinates of the perspective center. The object points can then be calculated as follows:

$$x = X_0 - c\left[\frac{r_{11}(X-X_0)+r_{12}(Y-Y_0)+r_{13}(Z-Z_0)}{r_{31}(X-X_0)+r_{32}(Y-Y_0)+r_{33}(Z-Z_0)}\right] \quad (2)$$

$$y = Y_0 - c\left[\frac{r_{11}(X-X_0)+r_{12}(Y-Y_0)+r_{13}(Z-Z_0)}{r_{31}(X-X_0)+r_{32}(Y-Y_0)+r_{33}(Z-Z_0)}\right] \quad (3)$$

The interior orientation defines the geometric parameters of the camera and the cone of the rays. By the end of the interior orientation, the metric characteristics of the camera calibration are calculated. The elements of the interior orientation are:

1) The camera's constant (c)
2) The Principal Point (x_0, y_0)
3) The distortion parameters like the Radial Distortions (Δr)

Specifically, the purpose of the interior orientation is to establish the relationship between a measurement system and the photo-coordinate system. So the value of 2 axes rotations, 2 axes scales and 2 shifts need to be calculated, in order to resolve the interior orientation.

A six parameter affine transformation as expressed in (4) can be employed for the interior orientating calculation. In the equations, the $\bar{x}, \bar{y}$ terms refer to the image system while the x, y coordinates refer to the camera's system.

$$\begin{aligned} x &= a_1\bar{x} + a_2\bar{y} + a_3 \\ y &= a_4\bar{x} + a_5\bar{y} + a_6 \end{aligned} \quad (4)$$

E. Coordinate transformation

Thereafter a simple transformation between the two coordinate systems (i.e., image to the 3D world space) is achieved using (Eq. (5) and (6) below). To aid understanding, fig. 6 depicts the transformation between the photo-coordinate system (k,v) and the object (3D space) coordinate system (X, Y, Z).

$$k = k_0 - c\left[\frac{r_{12}(X-X_0)+r_{22}(Y-Y_0)+r_{32}(Z-Z_0)}{r_{31}(X-X_0)+r_{32}(Y-Y_0)+r_{33}(Z-Z_0)}\right] \quad (5)$$

$$v = v_0 - c\left[\frac{r_{12}(X-X_0)+r_{22}(Y-Y_0)+r_{32}(Z-Z_0)}{r_{13}(X-X_0)+r_{23}(Y-Y_0)+r_{33}(Z-Z_0)}\right] \quad (6)$$

where c is the camera's constant (the vertical distance between the (X_0, Y_0, Z_0) and the film) and (k_0, v_0) is the projection of (X_0, Y_0, Z_0) on the photo-coordinate system. As before, r_{ij} are the elements of the 3D model and in this case, the elements describe the orientation of the capture in the 3d space, in relation with the object coordinate system (X, Y, Z). This elements can be described with the three angles ω, ϕ, κ. In addition, constant c is the vertical distance between the camera and the origin, point (X_0, Y_0, Z_0). Note that the relation between the object point coordinates (X, Y, Z) and the relative object coordinates on the image (k, v) resolve to the image coordinates.

The solution of (5) to X, Y is the following:

$$X = X_0 + (Z - Z_0)\left[\frac{r_{11}(k-k_0) + r_{12}(v-v_0) + r_{13}c}{r_{31}(k-k_0) + r_{32}(v-v_0) + r_{33}c}\right] \quad (7)$$

$$Y = Y_0 + (Z - Z_0)\left[\frac{r_{21}(k-k_0) + r_{22}(v-v_0) + r_{23}c}{r_{31}(k-k_0) + r_{32}(v-v_0) + r_{33}c}\right] \quad (8)$$

Equation (7) shows that every point of the object corresponds to only one point of the image. Equation (8) shows that in every image's point, correspond to infinitive points of the space, because of the Z dimension. This translated to the fact that having only one image does not allow for a 3D object to be reproduced. At least 2 images with the object be displayed on both is necessary. The above equations are necessary in order to understand the correlation of the two systems and how the 3rd dimension can be calculated if we have enough observations (known points in the photo-coordinate system). Figure 6 scematically presents the relation between the coordinates of the object on the images (k,v) and the coordinates of the object on the real world (X,Y,Z)

F. Photogrammetric products

The results that are provided by the completion of these two main steps, is an orthophoto of the area of interest, a 3d model, a DEM, and a dense cloud [7]. The orthophoto is a photograph which has been digitally manipulated and has therefore metric values. The important advantage of this model is that, when the user measures on it with a scale meter, he can recover all dimensions with the same precision as in a common diagram [10]. Doing so it can ensure the geometric accuracy of the displayed objects [19]. The orthophoto is geometrically identical with a map. The Digital Elevation Model (DEM) can be exported as a tiff file, which contains altitude values. The collected points from all the images compose a dense cloud that describes a three dimensional surface. The points are merged in order to create a model with a continuous surface. The dense cloud is the product, from which the two previous products can be created, so its accuracy is extremely important. Other photogrammetric products can be the surface profiles, topographic and special maps.

Currently there are various software packages containing the necessary steps to produce photogrammetric results. These software differ in their capabilities and limitations. Some

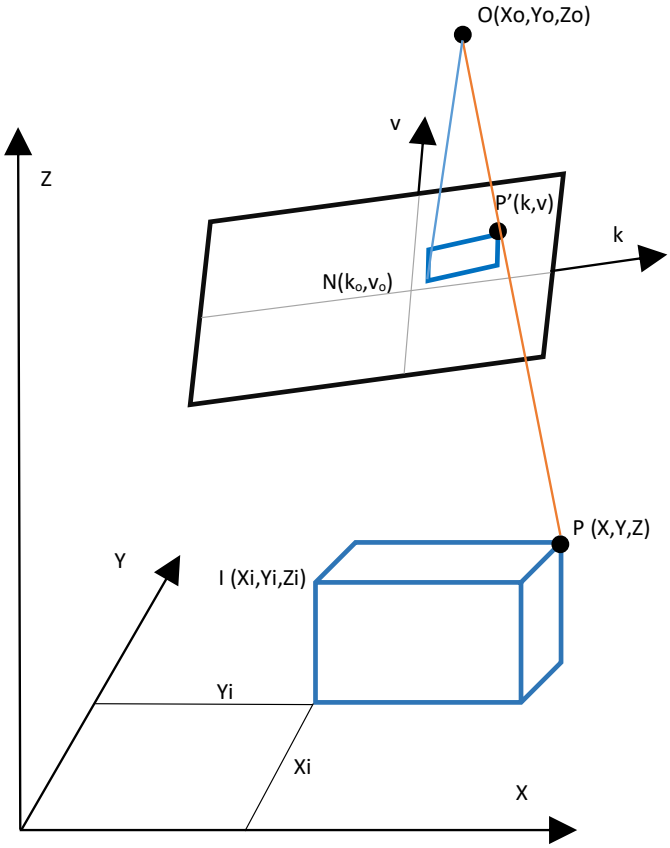

Fig. 6. The relation between the coordinates of the object on the images and the coordinates of the object on the real world. The blue cube appears on the image as a rectangle. The P(X,Y,Z) from the object space appears on the image as P'(k,v). The X,Y,Z axes refer to the object's coordinate system while the k,v refer to the photo-coordinate system.

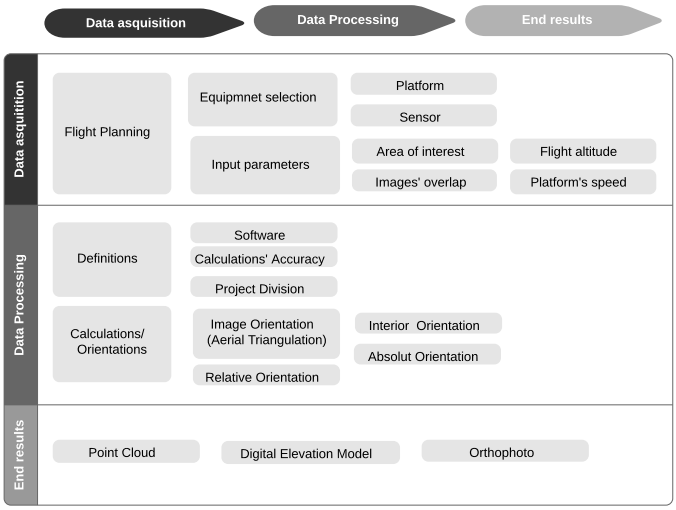

Fig. 7. The UAV photogrammetric procedure divided into 3 main sectors – Data acquisition, Data Processing, End results. In each sector, are attaching the middle decisions/parameters and steps that are needed to be done by this specific sequence.

of these packages are the Agisoft Metashape (commercial), pix4d (commercial), VisualSFM (open software), DroneMapper–RAPID version (open software), Open Drone Map (open software), GRAPHOS [28] (open software), Mic Mac (open software) [25]. The choice of the software should be done after assessing the capabilities and the limitations of each solution, since this will affect time, quality and the cost of the end result. Some of the above mentioned middle decisions and procedures are displayed in figure 7. For comparison purposes, this work considers both OpenDroneMap and the Agisoft Metashape. Open Drone Map can be used under the GPL license while Agisoft Metashape is a commercial software.

III. Proposed Methodology

The purpose of each survey project, has to lead to the decision of how the 2 main steps (i.e., flight planning and image processing) will be conducted based on the various parameters under consideration. Clearly, the needs and constrains of each survey mission reflect on the correct parameter values to be considered. Inaccurate parameter values could result to increased collection and processing times, and geographical model estimation errors. A survey can on one hand be considered holistically by processing the collected dataset in its unison to ensure quality [29] [30]. On the other hand, when time is of essence then the various steps of the photogrammetry procedure can be designed and executed in a parallel fashion. This work aims to investigate the latter fact and jointly consider flight planning parameters and the image processing procedure, in order to expedite the creation of the geographic model. Specifically, we investigate:

1) How the selection of the photogrammetric method parameters can affect the total mission time (different software tools are also investigated).
2) How the altitude can affect the total mission time and model quality.
3) How the division of the area into sectors can affect the total mission time.

Starting from the flight planning, there are several parameters for which one needs to decide. Firstly, is the decision about the sensors we need to install on the platform. Depending on their specifications (weight etc.), we have to select the platform. After that, depending on the needs and the purpose of the survey, the definition of some other parameters follows. These are the overlap of the images (if we need imaging data), the altitude of the flight, the area boundaries etc.

When the flight is finished, the image processing parameters are following. These are the decisions about the software, the accuracy (in case that the software offers this option), what photogrammetric products are needed to be created, if the process will be at once for all the images or not, the use of GCPs etc. Related to the image processing, the following steps take place:

1) Camera alignment. Including steps: Detecting Points, selecting pairs, matching points, estimating camera lo-

cation. The alignment gives as a result the tie points.

2) Dense point cloud generation. Including steps: Loading photos, depth maps generation, Dense point cloud generation. This gives as results the depth maps and the dense cloud.
3) Mesh & DEM. Including steps: Generating depth maps, processing depth maps, estimating surface, mesh generation. This gives a 3d model.
4) Orthophoto. This product is projected on a surface of a user choice (DEM, Dense Cloud).

As indicated before, we investigate both open source and commercial solutions (OpenDroneMap and Agisoft Metashape respectively) as the main photogrammetric packages, that establish relative camera positions, and use these positions to create accurate three-dimensional models of the ground surface. The models are then textured by draping the aerial photographs over them to produce photo-realistic three-dimensional rendered outputs of the ground surface [31].

IV. Experimental Results

A. Implementation Aspects

In order to investigate the experiments mentioned in the previous section, 12 flights were conducted. From these flights, images were gathered using the following setup.

TABLE I
FLIGHT SETTINGS

	Flight		
	A, B	C-E	F-L
Characteristics	Different areas, Same altitude	Same area, different altitude	Same area split into sectors, same altitude (combined to give total AOI)

For flights A/B, the images of two datasets were processed by the two photogrammetric packages, Agisoft Metashape and ODM and the total processing time was the primary performance indicator. Flights C, D, E were designed to investigate the impact of altitude on the processing time. The collected datasets from the respective flights captured images at 60m, 90m, 120m height. Finally, flights F-L have been conducted to investigate the total processing time when a particular area of interest is split into sectors. Specifically, flight F captured the full AOI area, while flights G and H split the AOI area into two equal sectors and flights I-L split the AOI area into 4 equal sectors.

The same aircraft and camera parameters have been used in all the flights. Specifically, DJI Mavic 2 Enterprise was employed with an onboard 12Mpixel camera and 82.6° FOV . Both the forward (p%) and the lateral (q%) overlap were fluctuated between 75%-80%. The collected data and associated parameters are depicted in table II.

The results presented hereafter are average values of processing the collected dataset several times using the same processing unit. Table III includes the results of the photogrammetric stages (DEM, Orthophoto etc.) using the commercial (Agisoft) and open source (OpenDroneMap) software tools for two distinct datasets. As indicated in the table, OpenDroneMap does not complete all stages of the photogrammetric product in order to produce the orthophoto, and this is the main reason for the significantly reduced execution time.

TABLE II
COLLECTED DATA

	Parameter					
	Flight	# of images	p%	q%	Alt. (m)	Res.
Value	A	54	75	75	50	4Kx2K
	B	49	80	80	120	4Kx2K
	C	143	85	85	60	4Kx2K
	D	73	85	85	90	4Kx2K
	E	49	85	85	120	4Kx2K
	F	326	85	85	40	4Kx2K
	G	186	85	85	40	4Kx2K
	H	182	85	85	40	4Kx2K
	I	122	85	85	40	4Kx2K
	J	94	85	85	40	4Kx2K
	K	109	85	85	40	4Kx2K
	L	110	85	85	40	4Kx2K

TABLE III
EXPERIMENT 1. TIME VS SOFTWARE

		Metashape	**ODM**
	Task	Time (s)	
Dataset A	Align	94,25	✓
	Dense Cloud	429,75	✓
	Mesh	3333,00	is non produced
	Texture	145,75	is non produced
	Tiled Model	690,25	✓
	DEM	7,00	is non produced
	Orthophoto	150,75	✓
	Total time (s)	4850,75	1020
	Task	Time (s)	
Dataset B	Align	102,33	✓
	Dense Cloud	2160,67	✓
	Mesh	4591,00	is non produced
	Texture	173,00	is non produced
	Tiled Model	356,67	✓
	DEM	3,00	is non produced
	Orthophoto	87,00	✓
	Total time (s)	7467,45	1620

It should be emphasized here that Metashape offers 6 levels of accuracy from which the 3rd (medium accuracy) had been selected to account for the results produced by ODM as well. The batch processing option of the Metashape had been selected so even though Metashape is not a command line tool, the process was automated to minimize interaction.

Table IV contains the results for varying flying altitudes and its effects on the time each photogrammetric product requires to complete. In this case, the data for all 3 flights (C-E) have been processed using Metashape. As shown in the table, the reduced number of images (143, 73, and 49, respectively) has an equally significant impact on the processing time, from 17325 down to 7521 seconds.

Table V contains the processing times when area sectorization is applied. Each column indicates the division of the area

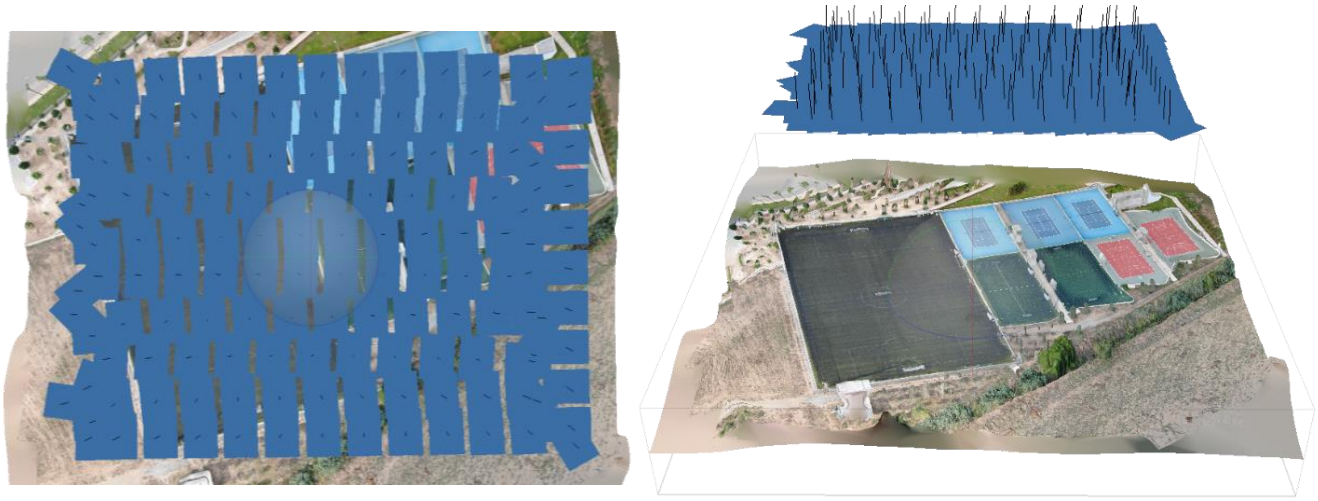

Fig. 8. Part of the UAV images processing in Metashape environment. The blue rectangles on the left, are a part of the taken images for the needs of the 2nd experiment. The black axes on them, represent the position that the platform had at the capture time and it is calculated with +-5m accuracy in the first stage. On the right, is shown the 3D Model which resulted by the 60m flight altitude.

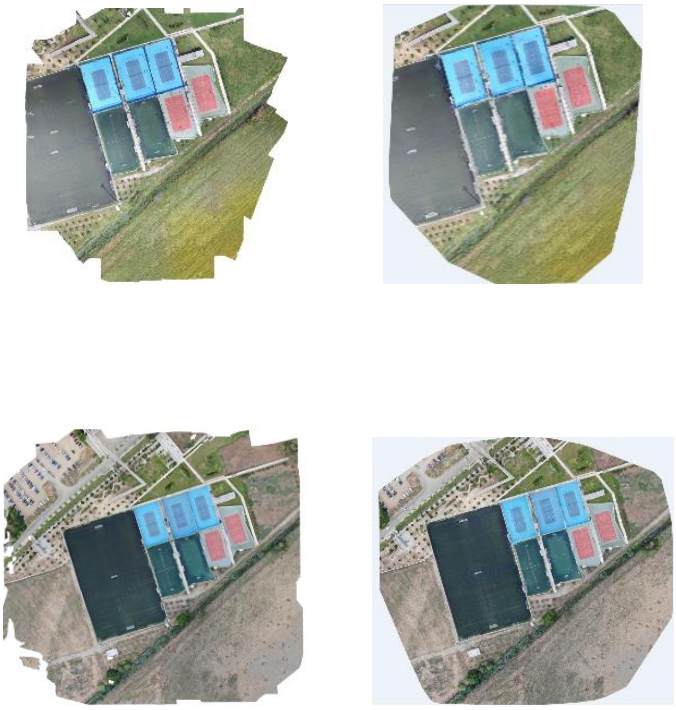

Fig. 9. The above 4 orthophotos have resulted by the end of the 1st experiment. On the 1st row are presenting the two orthophotos created by the Dataset A. On the left is the orthophoto created by the Agisoft Metashape and on the right is the orthophoto created by the same dataset by the OpenDroneMap. On the 2nd row, are presenting the orthophotos created by the two software, having as input the Dataset B

into the respective sectors and the index of each sector.

When the dataset covered the whole area of interest (a) the total completion time was about twice from the time of

TABLE IV
EXPERIMENT 2, TIME VS ALTITUDE.

Altitude (m)	60	90	120
Task		Time (s)	
Align	434,8	180,6	105,2
Dense Cloud	6796,4	2753,8	2172,8
Mesh	8593,2	4647,2	4570
Texture	435,6	239,4	174
Tiled Model	845,8	462,2	366,2
DEM	6,2	3,6	3,2
Orthophoto	212,8	150,2	129,8
Total time (s)	17324,8	8437	7521,2

TABLE V
EXPERIMENT 3. TIME VS # OF AREAS.

Area Division	Full area	Area/2 (2a)	Area/2 (2b)	Area/4 (4a)	Area/4 (4b)	Area/4 (4c)	Area/4 (4d)
Task				Time (s)			
Align	972,50	411,50	463,75	222,50	196,75	223,50	231,25
Dense Cloud	11274,75	6046,25	6427,75	3084,25	2413,25	3469,00	4698,50
Mesh	17100,00	10809,25	10185,00	4682,75	3416,75	4740,50	5887,25
Texture	710,00	414,75	405,50	275,00	215,00	255,25	256,50
Tiled Model	1293,50	789,00	762,75	590,50	487,75	531,25	448,50
DEM	13,75	7,25	6,25	6,00	4,75	4,25	4,25
Orthophoto	649,75	434,50	429,75	168,00	141,00	182,25	212,50
Total time (s)	32014,25	18912,50	18680,75	9029,75	6875,25	9406,00	11738,75

the subdivided area (2a, 2b). The same trend is also observed on the next datasets of the experiment which refer to the division of the whole area into 4 sectors. The sum of the total completion time of the last four datasets (4a-4d), has approximately the same value with the sum of the 2a and 2b datasets which is close enough with the value of the total completion time of the dataset refereed to the whole area (a). Importantly though, smaller sectors enable parallelization in the execution and thus significantly slash processing times.

V. CONCLUSION AND FUTURE WORK

In this paper we investigate control knobs for aerial survey using drone platforms. We investigate how parameters of

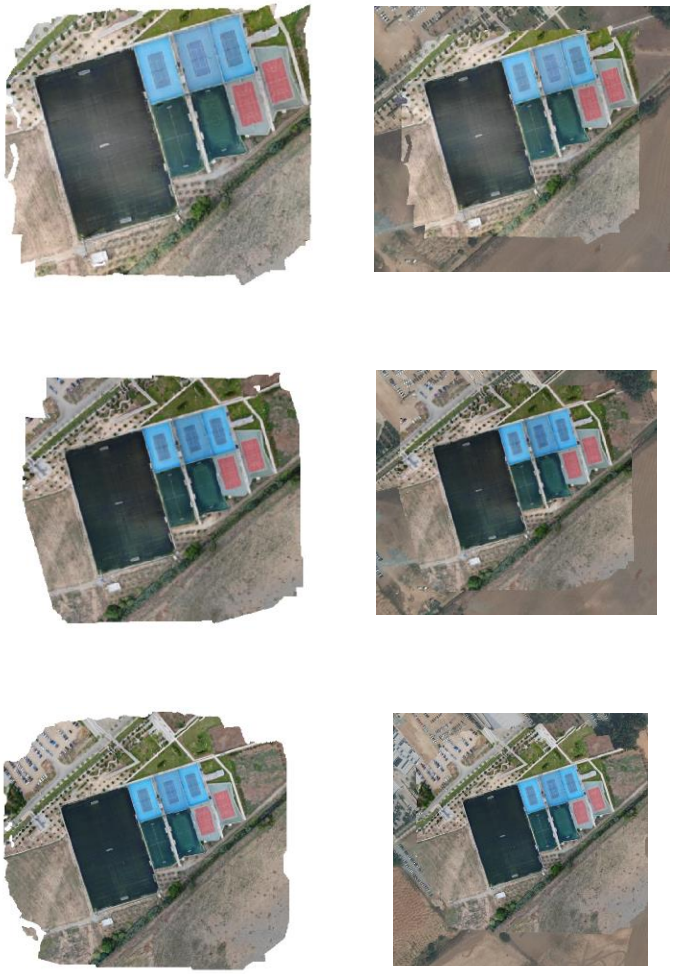

Fig. 10. The above orthophotos have resulted by the 2nd experiment. On the 1st column is displayed the orthophoto, whilst on the 2nd column a google satellite basemap has added. On the 1st row, is displayed the orthophoto created by the 60m-altitude flight, the 2nd row contains the orthophoto created by the 90m-altitude flight and the 3rd column presents the orthophoto created by the 120m-altitude flight.

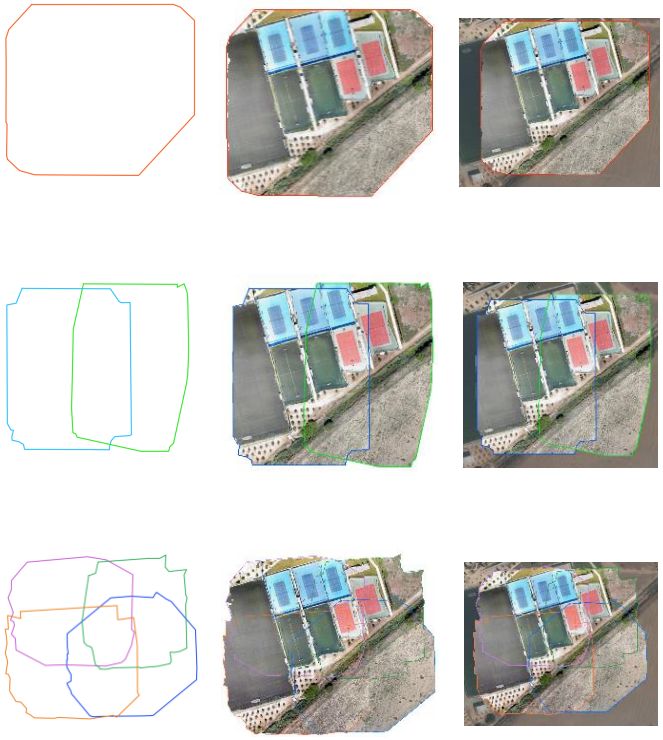

Fig. 11. The above orthophotos have resulted by the end of the 3rd experiment. The 1st column contains the boundaries of the covered area from each flight. On the 2nd column, the orthophotos created by each flight have added inside the area's boundaries, whilst on the 3rd column, a google satellite basemap has also added. The 1st row presents the orthophoto created by the flight covered the whole AOI at once, the 2nd row presents the 2 orthophotos created by 2 flights, whilst in the 3rd row are displayed the 4 orthophotos created by 4 flights, in order to cover the whole AOI by divide it into 4 subareas.

the photogrammetric procedure affect processing times and discuss ways to reduce completion times. Our investigation includes empirical findings from an extensive surveying campaign totalling 12 flights using various parameter settings (including altitude and coverage areas). In addition, a comparison of state-of-the-art commercial and open-source photogrammetric software was conducted to demonstrate the possible benefits in completion time from the use of different data processing algorithms. Through the analysis that followed we demonstrated the significant variations in completion time from the different approaches that are important to consider when designing time-sensitive surveys.

Future work will look at how the quality of the orthophotos can be regulated to further improve processing times. Note that in this work the output quality of the orthophotos was kept constant for fair comparison. Moreover, we plan to test additional photogrammetric software with the aim to better understand limitations and capabilities of the various algorithms employed.

ACKNOWLEDGEMENTS

This work is funded by the European Union Civil Protection under grant agreement No 782233 (LEAPFROG) and by the European Union's Horizon 2020 research and innovation programme under grant agreement No 739551 (KIOS CoE) and from the Republic of Cyprus through the Directorate General for European Programmes, Coordination and Development.

REFERENCES

[1] B. Kršák, P. Blišťan, A. Pauliková, P. Puškárová, L. Kovanič, J. Palková, and V. Zeliznaková, "Use of low-cost UAV photogrammetry to analyze the accuracy of a digital elevation model in a case study," *Measurement: Journal of the International Measurement Confederation*, vol. 91, pp. 276–287, 2016.

[2] Y. Vasuki, E. J. Holden, P. Kovesi, and S. Micklethwaite, "Semi-automatic mapping of geological Structures using UAV-based photogrammetric data: An image analysis approach," *Computers and Geosciences*, vol. 69, pp. 22–32, 2014. [Online]. Available: http://dx.doi.org/10.1016/j.cageo.2014.04.012

[3] M. Gerke and H. J. Przybilla, "Accuracy analysis of photogrammetric UAV image blocks: Influence of onboard RTK-GNSS and cross flight patterns," *Photogrammetrie, Fernerkundung, Geoinformation*, vol. 2016, no. 1, pp. 17–30, 2016.

[4] M. Uysal, A. S. Toprak, and N. Polat, "DEM generation with UAV Photogrammetry and accuracy analysis in Sahitler hill," *Measurement: Journal of the International Measurement Confederation*, vol. 73, pp. 539–543, 2015. [Online]. Available: http://dx.doi.org/10.1016/j.measurement.2015.06.010

[5] G. Zhou, "Near real-time orthorectification and mosaic of small UAV video flow for time-critical event response," *IEEE Transactions on Geoscience and Remote Sensing*, vol. 47, no. 3, pp. 739–747, 2009.

[6] F. Remondino, L. Barazzetti, F. Nex, M. Scaioni, and D. Sarazzi, "Uav Photogrammetry for Mapping and 3D Modeling – Current Status and Future Perspectives," *ISPRS - International Archives of the Photogrammetry, Remote Sensing and Spatial Information Sciences*, vol. XXXVIII-1/, no. January, pp. 25–31, 2012. [Online]. Available: http://www.int-arch-photogramm-remote-sens-spatial-inf-sci.net/XXXVIII-1-C22/25/2011/

[7] M. Gerke, "Developments in uav-photogrammetry," *Journal of Digital Landscape Architecture*, vol. 2018, pp. 262–272, 06 2018.

[8] F. Nex and F. Remondino, "UAV for 3D mapping applications: A review," *Applied Geomatics*, vol. 6, no. 1, pp. 1–15, 2014.

[9] "Accuracy of Unmanned Aerial Vehicle (UAV) and SfM photogrammetry survey as a function of the number and location of ground control points used," *Remote Sensing*, vol. 10, no. 10, 2018.

[10] S. Hawkins, "Using a drone and photogrammetry software to create orthomosaic images and 3D models of aircraft accident sites," *Isasi*, no. October, pp. 1–26, 2016.

[11] A. R. Yusoff, M. F. Mohd Ariff, K. M. Idris, Z. Majid, and A. K. Chong, "Camera calibration accuracy at different UAV flying heights," *International Archives of the Photogrammetry, Remote Sensing and Spatial Information Sciences - ISPRS Archives*, vol. 42, no. 2W3, pp. 595–600, 2017.

[12] M. Półka, S. Ptak, Ł. Kuziora, and A. Kuczyńska, "The Use of Unmanned Aerial Vehicles by Urban Search and Rescue Groups," *Drones - Applications*, no. September, 2018.

[13] D. Giordan, A. Manconi, F. Remondino, and F. Nex, "Use of unmanned aerial vehicles in monitoring application and management of natural hazards," *Geomatics, Natural Hazards and Risk*, vol. 8, no. 1, pp. 1–4, 2017. [Online]. Available: https://doi.org/10.1080/19475705.2017.1315619

[14] B. Ruzgiene, T. Berteška, S. Gečyte, E. Jakubauskiene, and V. Č. Aksamitauskas, "The surface modelling based on UAV Photogrammetry and qualitative estimation," *Measurement: Journal of the International Measurement Confederation*, vol. 73, pp. 619–627, 2015.

[15] H. Eisenbeiss, "Applications of photogrammetric processing using an autonomous model helicopter," *Revue Francaise de Photogrammetrie et de Teledetection*, no. 185, pp. 51–56, 2007.

[16] S. P. Yeong, M. King, and S. S. Dol, "A Review on Marine Search and Rescue Operations Using Unmanned Aerial Vehicles," *World Academy of Science, Engineering and Technology International Journal of Marine and Environmental Sciences*, vol. 9, no. 2, pp. 396–399, 2015. [Online]. Available: https://waset.org/publications/10001953/a-review-on-marine-search-and-rescue-operations-using-unmanned-aerial-vehicles

[17] B. Rao, A. G. Gopi, and R. Maione, "The societal impact of commercial drones," *Technology in Society*, vol. 45, pp. 83 – 90, 2016. [Online]. Available: http://www.sciencedirect.com/science/article/pii/S0160791X15300828

[18] M. Marsella, C. Nardinocchi, C. Proietti, L. Daga, and M. Coltelli, "Monitoring active volcanos using aerial images and the orthoview tool," *Remote Sensing*, vol. 6, no. 12, pp. 12 166–12 186, 2014.

[19] Y. Liu, X. Zheng, G. Ai, Y. Zhang, and Y. Zuo, "Generating a high-precision true digital orthophoto map based on UAV images," *ISPRS International Journal of Geo-Information*, vol. 7, no. 9, 2018.

[20] K. Bartoš, K. Pukanská, and J. Sabová, "Overview of Available Open-Source Photogrammetric Software, its Use and Analysis," *International Journal for Innovation Education and Research www.ijier.net*, vol. 2, no. May 2017, pp. 62–70, 2014.

[21] J. Casaca and M. J. Henriques, "The Geodetic Surveying Methods in the Monitoring of Large Dams in The Geodetic Surveying Methods in the Monitoring of Large Dams in Portugal," *Civil Engineering*, no. April 2002, pp. 1–12, 2002.

[22] M. BONDREA, S. NAȘ, R. FĂRCAȘ, M. DÎRJA, and P. Sestras, "Construction survey and precision analysis using rtk technology and a total station at axis stake-out on a construction site," 06 2016.

[23] J. Straub, B. Kading, A. Mohammad, and S. Kerlin, "Characterization of a Large, Low-Cost 3D Scanner," *Technologies*, vol. 3, no. 1, pp. 19–36, 2015.

[24] R. Jiang, D. V. Jáuregui, and K. R. White, "Close-range photogrammetry applications in bridge measurement: Literature review," *Measurement: Journal of the International Measurement Confederation*, vol. 41, no. 8, pp. 823–834, 2008.

[25] E. Rupnik, M. Daakir, and M. Pierrot Deseilligny, "MicMac – a free, open-source solution for photogrammetry," *Open Geospatial Data, Software and Standards*, vol. 2, no. 1, 2017.

[26] M. Koeva, M. Muneza, C. Gevaert, M. Gerke, and F. Nex, "Using UAVs for map creation and updating. A case study in Rwanda," *Survey Review*, vol. 50, no. 361, pp. 312–325, 2018. [Online]. Available: https://doi.org/10.1080/00396265.2016.1268756

[27] E. E. Elnima, "A solution for exterior and relative orientation in photogrammetry, a genetic evolution approach," *Journal of King Saud University - Engineering Sciences*, vol. 27, no. 1, pp. 108 – 113, 2015. [Online]. Available: http://www.sciencedirect.com/science/article/pii/S1018363913000196

[28] D. Gonzalez-Aguilera, L. López-Fernández, P. Rodriguez-Gonzalvez, D. Hernandez-Lopez, D. Guerrero, F. Remondino, F. Menna, E. Nocerino, I. Toschi, A. Ballabeni, and M. Gaiani, "GRAPHOS – open-source software for photogrammetric applications," *Photogrammetric Record*, vol. 33, no. 161, pp. 11–29, 2018.

[29] G. Vacca, A. Dessì, and A. Sacco, "The use of nadir and oblique UAV images for building knowledge," *ISPRS International Journal of Geo-Information*, vol. 6, no. 12, 2017.

[30] C. Xing, J. Wang, and Y. Xu, "Overlap analysis of the images from unmanned aerial vehicles," *Proceedings - International Conference on Electrical and Control Engineering, ICECE 2010*, no. June 2010, pp. 1459–1462, 2010.

[31] J. Quartermaine, B. Olson, and M. Howland, "Appendix b: Using photogrammetry and geographic information systems (gis) to draft accurate plans of qazion," *Journal of Eastern Mediterranean Archaeology Heritage Studies*, vol. 1, pp. 169–174, 01 2013.